Time-Resolved Stochastic Dynamics of Quantum Thermal Machines

Abhaya S. Hegde,[1,*] Patrick P. Potts,[2,†] and Gabriel T. Landi[1,‡]
[1]*Department of Physics and Astronomy, University of Rochester, Rochester, New York 14627, USA*
[2]*Department of Physics and Swiss Nanoscience Institute, University of Basel, Klingelbergstrasse 82 CH-4056, Switzerland*

(Received 20 August 2024; revised 4 December 2024; accepted 25 March 2025; published 15 April 2025)

Steady-state quantum thermal machines are typically characterized by a continuous flow of heat between different reservoirs. However, at the level of discrete stochastic realizations, heat flow is unraveled as a series of abrupt quantum jumps, each representing an exchange of finite quanta with the environment. In this work, we present a framework that resolves the dynamics of quantum thermal machines into cycles classified as enginelike, coolinglike, or idle. We analyze the statistics of individual cycle types and their durations, enabling us to determine both the fraction of cycles useful for thermodynamic tasks and the average waiting time between cycles of a given type. Central to our analysis is the notion of intermittency, which captures the operational consistency of the machine by assessing the frequency and distribution of idle cycles. Our framework offers a novel approach to characterizing thermal machines, with significant relevance to experiments involving mesoscopic transport through quantum dots.

DOI: 10.1103/PhysRevLett.134.150402

Introduction—A typical quantum thermal machine consists of a system situated between hot and cold thermal baths, extracting or absorbing energy in the form of work, as depicted in Fig. 1 [1–5]. As an engine, it extracts work while transferring heat from hot to cold; as a refrigerator, it absorbs work to move heat from cold to hot. In autonomous machines, this is usually pictured as a continuous process, where heat and work constantly flow through the system [6–8]. However, within the microscopic domain, the stochastic nature of system and bath interactions endows an alternative perspective where energy is exchanged with the baths in the form of abrupt jumps. This is the basis for stochastic thermodynamics in classical (Pauli) rate equations [9–11], as well as quantum models in the quantum jumps formalism [12–23].

The jumps occur at random times and in random "channels." Let us broadly classify these channels as either an injection (I) or an extraction (E) of energy into or out of a system induced by hot (h) or cold (c) baths, resulting in four distinct types of monitored channels $\mathbb{M} = \{I_h, E_h, I_c, E_c\}$. Generalizing to multiple injection and extraction channels per bath is straightforward. The quantum trajectory of such a machine, in the quantum jump unraveling, appears as a random string, e.g.,

$$I_h E_c I_c I_h E_h E_c I_h I_c E_h I_c \ldots, \tag{1}$$

along with their timestamps $t_1, t_2, \ldots$, indicating when each jump occurred. This representation of the dynamics is grounded in several experimental observations either through direct detection of jumps [24–26] or by monitoring the states continuously to deduce the jump processes driving the observed state transitions [27–35]. Note that only heat exchange events with the environment are included in (1), as work events, typically associated with unitary drives are assumed undetectable [1].

The central question we address in this work is, can specific thermodynamic cycles be identified solely from strings like (1) so that their statistics can be explored?

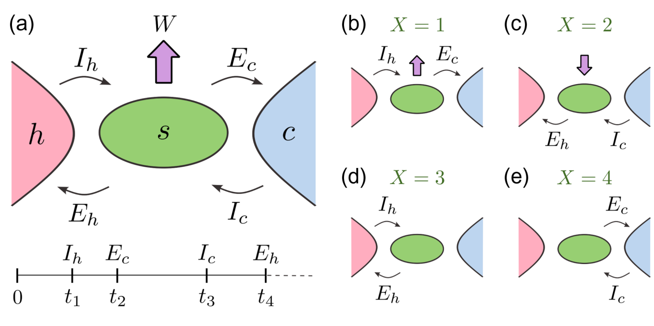

FIG. 1. (a) In a quantum thermal machine (s), heat injection (I) and extraction (E) are mediated by hot (h) and cold (c) reservoirs, represented as random events occurring at random times within the quantum jump unraveling. (b)–(e) These jumps can be categorized into four cycles denoted by pairs $I_{\bullet}E_{\bullet}$ and labeled by X. (b) Work extraction cycle ($X = 1$): Heat is transferred from hot to cold bath, extracting work. (c) Cooling cycle ($X = 2$): Excitations move from cold to hot bath, consuming work. These are useful cycles. (d),(e) Idle cycles ($X = 3, 4$): No heat transfer occurs overall.

*Contact author: a.hegde@rochester.edu
†Contact author: patrick.potts@unibas.ch
‡Contact author: gabriel.landi@rochester.edu

For instance, one might intuitively characterize the sequence I_cE_h as a refrigeration cycle, since an energy quanta was injected from c to the system, and subsequently extracted to h suggesting work consumption. Similarly, I_hE_c could be seen as an enginelike process (or accelerator [36]). These are both examples of "useful cycles." Conversely, pairs such as I_hE_h and I_cE_c are events that fail to peddle quanta of energy overall, and incur no entropy production. We refer to these as "idle cycles." While a machine might operate as an engine on average, the stochastic nature of these processes manifests in individual realizations yielding different cycles [37,38].

Classifying cycles raises several meaningful questions, such as the following: What is the probability of each type of cycle? How are cycles related to steady-state currents? What is the time required to complete each cycle? How many idle cycles precede a useful one?

These questions relate to the extensive literature on full counting statistics (FCS) [39–41], fluctuation theorems [42–49], and thermodynamical aspects of quantum trajectories [50–52]. Addressing them involves exploring time-resolved and cycle-resolved quantities, offering a fine-grained understanding of the dynamics.

In attempting to classify cycles this way, a challenge arises when the system can withhold multiple excitations at once. For instance, in the string (1), what meaning should be ascribed to the substring $I_cI_hE_hE_c$? Because excitations are indistinguishable, it is impossible to infer if this was $I_cI_hE_hE_c$ (two idles) or $I_cI_hE_hE_c$ (a refrigeration followed by an engine cycle). While this is not an issue as far as the average heat and work currents are concerned, it does cause ambiguity in defining time-resolved quantities. In this Letter, we focus on systems that can retain only one excitation at a time; i.e., when injections and extractions alternate ($I_\bullet E_\bullet I_\bullet E_\bullet\ldots$) in the trajectory. This assumption is common in experiments involving single [32–34] or double [53–57] quantum dots in the Coulomb blockade regime, as well as realizations of quantum heat engines [58,59].

First, we establish the restrictions imposed by the single-excitation hypothesis on a quantum Markovian master equation. Then, we employ the tools of waiting time distributions of the quantum jump unraveling [21–23] to fully characterize the statistics of cycles. Finally, we illustrate our results with a three-level maser example.

Theory—We consider a finite-dimensional system weakly coupled to hot and cold baths. Work may be performed either by a driven Hamiltonian $H(t)$ or by additional work reservoirs. It is assumed that the dynamics can be described by a quantum master equation [60,61] ($\hbar = k_B = 1$ throughout),

$$\frac{d\rho}{dt} = \mathcal{L}_t\rho \equiv -i[H(t),\rho] + \sum_n \mathcal{D}[K_n]\rho + \sum_{\alpha\in\{h,c\},j}\Big(\gamma^-_{\alpha j}\mathcal{D}[L_{\alpha j}] + \gamma^+_{\alpha j}\mathcal{D}[L^\dagger_{\alpha j}]\Big)\rho, \quad (2)$$

where $\mathcal{D}[L]\rho = L\rho L^\dagger - \frac{1}{2}\{L^\dagger L,\rho\}$. Here, $\{L_{\alpha j}\}$ are jump operators for the hot ($\alpha = h$) and cold ($\alpha = c$) baths, with $L_{\alpha j}$ denoting extractions and $L^\dagger_{\alpha j}$ denoting injections, each occurring at rates $\gamma^\mp_{\alpha j}$, respectively. Finally, K_n are jump operators of work reservoirs, which are often used in describing absorption refrigerators [62–66].

We assume one can only monitor whether energy is injected (extracted) from (to) the hot or cold baths without identifying the specific jump operator (indexed by j) responsible. Therefore, the four corresponding jump superoperators are

$$\mathcal{J}_{E_\alpha}\rho = \sum_j \gamma^-_{\alpha j} L_{\alpha j}\rho L^\dagger_{\alpha j}, \qquad \mathcal{J}_{I_\alpha}\rho = \sum_j \gamma^+_{\alpha j} L^\dagger_{\alpha j}\rho L_{\alpha j}. \quad (3)$$

As our first result, we prove in Supplemental Material [67] that the condition for the quantum trajectory to have alternating injections and extractions (i.e., at most a single excitation) is achieved, if and only if, there exist two subspaces $\mathcal{H}_E$ and $\mathcal{H}_I$ spanning the system Hilbert space $\mathcal{H}$, such that

$$L_{\alpha j} = \mathcal{P}_E L_{\alpha j}\mathcal{P}_I \quad \forall\ \alpha, j; \quad (4a)$$

$$\mathcal{P}_E H(t)\mathcal{P}_I = \mathcal{P}_I H(t)\mathcal{P}_E = 0; \quad (4b)$$

$$\mathcal{P}_E K_n\mathcal{P}_I = \mathcal{P}_I K_n\mathcal{P}_E = 0, \quad (4c)$$

where $\mathcal{P}_{E/I}$ are projection operators onto $\mathcal{H}_{E/I}$, satisfying $\mathcal{P}_E + \mathcal{P}_I = 1$. Thus, the jump operators of the baths must be block upper triangular, while those of the work reservoir, and Hamiltonian must be block diagonal in the basis spanned by the states in the subspaces $\mathcal{H}_E$ and $\mathcal{H}_I$.

Consequently, $L_{\alpha j}$ takes the system to $\mathcal{H}_E$ by extracting energy, while $L^\dagger_{\alpha j}$ directs it to $\mathcal{H}_I$ by injecting energy. We refer to $\mathcal{H}_E$ and $\mathcal{H}_I$ as postextraction and postinjection subspaces. While the unitary dynamics and work reservoirs can inject (extract) work into (out of) the system, this result implies that such processes must occur within each subspace. Transitions between these subspaces are only feasible through interactions with the baths. An example is the three-level maser [see Fig. 2(a)]; other examples are hinted at in Ref. [67].

We henceforth assume, as is often the case, that there exists a rotating frame where $H(t)$ is time independent, and that the steady state ($\mathcal{L}\rho_{\rm ss} = 0$) in this frame is unique. The single-excitation hypothesis implies a conservation law for the average excitation current exchanged with the baths,

$$\mathcal{I}_{\rm ex} \coloneqq \mathrm{tr}\{(\mathcal{J}_{E_c} - \mathcal{J}_{I_c})\rho_{\rm ss}\} = -\mathrm{tr}\{(\mathcal{J}_{E_h} - \mathcal{J}_{I_h})\rho_{\rm ss}\}, \quad (5)$$

which is deduced by noting that $(d/dt)\mathrm{tr}\{\mathcal{P}_E\rho(t)\mathcal{P}_E\} \to 0$ as the system approaches the steady state. Equation (5) does not imply that the heat currents to both baths are equal, as jumps to each bath generally involve different energies. Indeed, their mismatch accounts for the work exchanged. This current is often related to energy fluxes and entropy production rates.

Statistics of cycles—Under the single-excitation assumption, the trajectories analogous to (1) can be characterized in terms of the statistics of four possible pairs: I_hE_c, I_cE_h, I_hE_h, and I_cE_c. We refer to each pair $I_\bullet E_\bullet$ as a "cycle" and label them as $X = 1, 2, 3, 4$, respectively (see Fig. 1). $X = 1$ is a work extraction cycle [72] and $X = 2$ a refrigeration cycle, while $X = 3, 4$ are idle cycles.

We are interested in the long-time steady-state behavior of strings of the form $X_1X_2\ldots = I_\bullet E_\bullet I_\bullet E_\bullet\ldots$, adopting the convention that strings always begin with an injection. Then, as explained in Ref. [67], the probability of observing a specific sequence $X_1,\ldots,X_n$, with durations $\tau_1,\ldots,\tau_n$, is given by

$$p_{X_1,\ldots,X_n}(\tau_1,\ldots,\tau_n) = \mathrm{tr}\{\mathcal{O}_{X_n,\tau_n}\ldots\mathcal{O}_{X_1,\tau_1}\pi_E\}, \tag{6}$$

where

$$\mathcal{O}_{X,\tau} \equiv \int_0^\tau dt\, \mathcal{J}_{E_X} e^{\mathcal{L}_0(\tau-t)} \mathcal{J}_{I_X} e^{\mathcal{L}_0 t}, \tag{7}$$

and $\mathcal{L}_0 = \mathcal{L} - \sum_\alpha(\mathcal{J}_{E_\alpha} + \mathcal{J}_{I_\alpha})$ is the no-jump superoperator. In Eq. (6), we have introduced the jump steady state [67,73]

$$\pi_E = \frac{(\mathcal{J}_{E_h} + \mathcal{J}_{E_c})\rho_{\mathrm{ss}}}{\mathrm{tr}\{(\mathcal{J}_{E_h} + \mathcal{J}_{E_c})\rho_{\mathrm{ss}}\}} \in \mathcal{H}_E, \tag{8}$$

to ensure the jump sequence is stationary.

Marginalizing Eq. (6) over all (X_i, τ_i) except one yields the probability that a single cycle is of type X and duration τ,

$$p_X(\tau) = \mathrm{tr}\{\mathcal{O}_{X,\tau}\pi_E\}. \tag{9}$$

Integrating over τ yields the probability that the cycle is of type X:

$$p_X = \int_0^\infty d\tau\, p_X(\tau) = \mathrm{tr}\{\mathcal{O}_X\pi_E\}, \tag{10}$$

where $\mathcal{O}_X = \int_0^\infty d\tau\, \mathcal{O}_{X,\tau} = \mathcal{J}_{E_X}\mathcal{L}_0^{-1}\mathcal{J}_{I_X}\mathcal{L}_0^{-1}$, with $\sum_{X=1}^4 p_X = 1$.

The average cycle time given it is of type X reads as

$$E(\tau|X) = \frac{1}{p_X}\int_0^\infty d\tau\, \tau p_X(\tau). \tag{11}$$

In Ref. [67], we show

$$E(\tau) = \sum_{X=1}^4 E(\tau|X)p_X = \frac{2}{\mathcal{K}_{hc}}, \tag{12}$$

where $\mathcal{K}_{hc}$ is the dynamical activity of the baths representing the average number of jumps per unit time in the steady state. This activity is closely tied to the kinetic uncertainty relation [74], and for a classical Markov process, it also relates to information geometry [75].

The probabilities in Eq. (10) represent the relative occurrence of each cycle type over many trajectories, regardless of their duration. In Ref. [67], we prove that $p_{1/2}$ and the excitation current from Eq. (5) are related by

$$\mathcal{I}_{\mathrm{ex}} = \frac{p_1 - p_2}{E(\tau)}, \tag{13}$$

which provides a fundamental connection between usual steady-state currents and our results: the system functions as an engine when $p_1 > p_2$, and as a refrigerator when $p_1 < p_2$.

Example: Three-level system—We apply our results to a three-level maser [1,70,71,76–82] whose schematic is depicted in Fig. 2. It is coupled to hot and cold baths at energy ω_α and temperature T_α with their populations following a Bose-Einstein distribution given by $\bar{n}_\alpha = [\exp(\omega_\alpha/T_\alpha) - 1]^{-1}$. The maser is driven by the Hamiltonian $H(t) = (\omega_h - \omega_c)\sigma_{11} + \omega_h\sigma_{22} + \epsilon(e^{i\omega_d t}\sigma_{01} + e^{-i\omega_d t}\sigma_{10})$ with a Rabi drive of strength ϵ and frequency ω_d. The jump operators are $L_h = \sigma_{02}$, $L_c = \sigma_{12}$ (and $K_n = 0$) with rates $\gamma_\alpha^- = \gamma_\alpha(\bar{n}_\alpha + 1)$ and $\gamma_\alpha^+ = \gamma_\alpha\bar{n}_\alpha$. Here, $\sigma_{ij} = |i\rangle\langle j|$ are the transition operators. The postextraction subspace is spanned by $\{|0\rangle, |1\rangle\}$, and the postinjection by $\{|2\rangle\}$. As anticipated, the Hamiltonian is block diagonal in the joint basis of these subspaces.

Figure 3(a) illustrates $p_X(\tau)$ from Eq. (9) [see Ref. [67] for explicit expressions]. For large τ, these probabilities scale as

$$p_X(\tau) \sim e^{-\Gamma\tau}\left[1 + C_X\cos\left(2\tau\sqrt{\epsilon^2 + \frac{\Delta^2 + \Lambda^2}{4}} + \phi_X\right)\right], \tag{14}$$

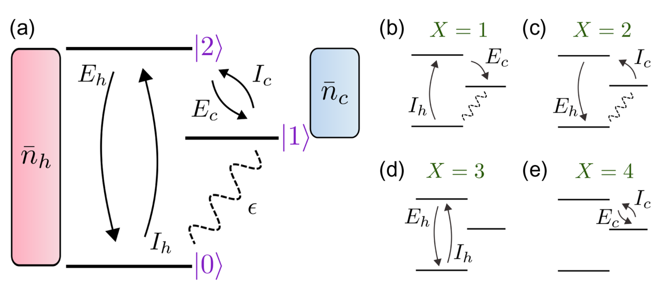

FIG. 2. (a) Schematic of a three-level maser connected to hot and cold baths and driven by a Rabi drive, illustrating the four jump processes induced by the baths. (b)–(e) All four cycles for this model akin to Figs. 1(b)–1(e).

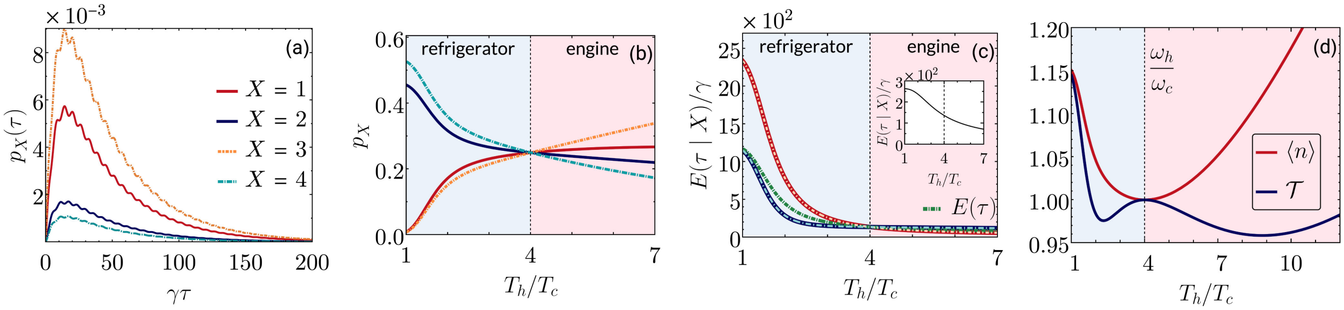

FIG. 3. (a)–(d) Statistics of cycles in three-level maser from Fig. 2. (a) Probability of observing a cycle X within a duration τ [Eq. (9)] at resonance $\omega_d = \omega_h - \omega_c$ and $T_h/T_c = 10$. (b) Total probability of observing a cycle X [Eq. (10)] and (c) expectation values for cycle duration [Eqs. (11) and (12)] as a function of the ratio of bath temperatures. A vertical line at $T_h/T_c = \omega_h/\omega_c$ separates the refrigerator and engine regimes. The inset shows all expectation values nearly converge at resonance. (d) Mean of intervening idle cycles between useful cycles and ratios of fraction of idle-to-useful times against bath gradient. The parameters are fixed (in units of $T_c = 1$) at $\gamma_h = \gamma_c \equiv \gamma = 0.05$, $\omega_h = 8$, $\omega_c = 2$, $\omega_d = 4$, $\epsilon = 0.5$ unless mentioned otherwise.

where $\Gamma = (\bar{n}_h\gamma_h + \bar{n}_c\gamma_c)/2$ is the net decoherence rate, $\Lambda = (\bar{n}_h\gamma_h - \bar{n}_c\gamma_c)/2$ indicates the bias, $\Delta = (\omega_h - \omega_c) - \omega_d$ is the detuning, and C_X, ϕ_X are constants determined by parameters of this model. The oscillatory behavior reflects the coherent drive, reminiscent of Rabi oscillations between $|0\rangle$ and $|1\rangle$, while the exponential decay captures the stochastic nature of jump events.

The marginals p_X from Eq. (10) are shown in Fig. 3(b) as a function of the ratio T_h/T_c. The plot highlights the different regimes of operation, which changes from refrigeration to engine at $T_h/T_c = \omega_h/\omega_c$. It is noteworthy that [67]

$$p_1 - p_2 \propto \bar{n}_h - \bar{n}_c, \qquad \frac{p_3}{p_1} = \frac{p_2}{p_4} = \frac{(\bar{n}_h + 1)\gamma_h}{(\bar{n}_c + 1)\gamma_c}, \tag{15}$$

implying that, when $\gamma_h = \gamma_c$, the probabilities of idle cycles bound those of useful ones across all parameter ranges. As a result, it is always more likely to observe the machine undergoing a cycle with no net heat transfer.

The average cycle durations [Eqs. (11) and (12)] are plotted in Fig. 3(c); for this model, it turns out that $E(\tau|1) = E(\tau|3)$ and $E(\tau|2) = E(\tau|4)$. Noticeably, the cycles tend to take much longer in the refrigeration regime. Moreover, at resonance, all conditional averages tend to become very close (although not strictly equal), as shown in the inset of Fig. 3(c). For small ϵ, the probability of useful cycles $p_u \coloneqq p_1 + p_2$ scales as $\epsilon^2/(\Gamma^2 + \Delta^2)$. This highlights that stronger pumps, more resonant drives, and lower damping favor useful cycles.

In this model, the excitation current from Eq. (13) is directly related to the steady-state heat, work, and entropy production currents, as $\dot{Q}_h = \omega_h\mathcal{I}_{\mathrm{ex}}$, $\dot{Q}_c = -\omega_c\mathcal{I}_{\mathrm{ex}}$, $\dot{W} = \omega_d\mathcal{I}_{\mathrm{ex}}$, and $\dot{\Sigma} = \sigma\mathcal{I}_{\mathrm{ex}}$, where $\sigma = \omega_c/T_c - \omega_h/T_h$. The second law $\dot{\Sigma} \geq 0$ confirms the conditions for engine and refrigeration regimes, depending on the sign of σ.

On the level of individual stochastic events, idle cycles ($X = 3$, 4) are entropy neutral, while engine ($X = 1$) and refrigeration ($X = 2$) cycles produce entropy $\pm\sigma$, respectively. The average entropy produced per cycle is therefore $E(\Sigma_{\mathrm{cyc}}) = \sigma(p_1 - p_2)$, which relates to the steady-state entropy production rate as $\dot{\Sigma} = E(\Sigma_{\mathrm{cyc}})/E(\tau)$. The variance in entropy production within each cycle reads

$$\mathrm{Var}(\Sigma_{\mathrm{cyc}}) = \sigma^2[(1 - p_{\mathrm{id}}) - (p_1 - p_2)^2], \tag{16}$$

where $p_{\mathrm{id}} \coloneqq p_3 + p_4$ is the probability of idle cycles. This variance vanishes in the absence of coherent drive ($\epsilon = 0$ implying $p_{\mathrm{id}} = 1$, $p_1 = p_2 = 0$) and is bounded by $\sigma^2(1 - p_{\mathrm{id}})$ when $p_1 = p_2$. Thus, the fluctuations in entropy production are directly related to how often the machine fails to produce useful cycles.

Intermittency of a machine—These findings show that thermodynamic quantities can vary significantly between individual cycles, highlighting the role of the machine's regularity or intermittency in its performance. Despite this variability, due to $\dot{Q}_h = \omega_h\mathcal{I}_{\mathrm{ex}}$ and $\dot{Q}_c = -\omega_c\mathcal{I}_{\mathrm{ex}}$, these fluctuations leave the steady-state efficiency unaffected, with $\eta = 1 + \dot{Q}_c/\dot{Q}_h = 1 - \omega_c/\omega_h$. This perspective aligns with Ref. [83], wherein the need for a complementary metric to characterize small-scale machines was suggested.

Intermittency as a measure should capture the distribution of idle cycles as a proxy for consistency in heat flow. Concretely, intermittency can be characterized by the average number of idle cycles between two useful ones. Since the typical thermodynamic variables cannot witness idle cycles, their presence is inferred from only the time the machine spends abstained from transferring heat. Thus, in a manner analogous to the previous definition, the average fraction of time spent performing idle cycles provides another aspect of intermittency, particularly when idle cycles occur on a different timescale than useful ones. A perfectly regular machine—one where only useful cycles occur—would have zero intermittency.

For the three-level maser, characterizing intermittency is greatly simplified since cycles are independent. In other words, these cycles form renewal processes. The trajectory probability from Eq. (6) factors into a product because the postinjection subspace is a singleton ($|2\rangle$). The average number of idles n between useful ones, and the fraction representing the average time spent in idle cycles relative to useful cycles $\mathcal{T}$ appear as [67]

$$\langle n\rangle = \frac{p_{\mathrm{id}}}{p_u} = \frac{p_3+p_4}{p_1+p_2}, \quad \mathcal{T} = \frac{p_3 E(\tau|3) + p_4 E(\tau|4)}{p_1 E(\tau|1) + p_2 E(\tau|2)}, \tag{17}$$

both of which are plotted in Fig. 3(d). Assuming $\gamma_h = \gamma_c$, we find $\langle n\rangle \geq 1$ and thus the machine operates irregularly. Selecting an appropriate ratio of bath temperatures, e.g., $T_h/T_c \sim 9$, enables quicker cycle completion but results in a higher participation of idle cycles. This emphasizes the subtle trade-offs involved in balancing two aspects of intermittency. This trade-off is further illuminated by examining the distributions of idle and useful cycle times as explored in Ref. [67]. Moreover, the framework in Ref. [67] generalizes to machines with correlated cycles, capturing dynamics beyond independent renewal processes.

Conclusions—We showed how to unravel the time-dependent statistics of quantum thermal machines, enabling classification of stochastic dynamics into distinct cycles based on how they interact with different resource reservoirs, determination of cycle occurrence frequencies, and cycle durations. Our results encompass all statistical correlations between cycles, and also connect with known results in FCS for the average excitation current and dynamical activity. This approach provides a new avenue for characterizing quantum thermal machines using experimentally accessible data. In particular, our formalism could be readily employed to analyze, e.g., mesoscopic transport in quantum dot experiments shedding light on the underlying thermodynamics and emphasizing the role of regularity in heat flow.

A key takeaway from this analysis is the concept of intermittency, i.e., the reliability of a machine in performing thermodynamically useful tasks. Since our approach enables the identification of both useful and idle cycles, we now have the tools to optimize the intermittency for fixed efficiency and output power. Our results also allow us to examine cycle "bunching," specifically how the occurrence of one useful cycle influences the probability of observing another. These insights have the potential to significantly deepen our understanding and interpretation of quantum stochastic processes.

Acknowledgments—The authors express thanks to Joseph Smiga, Felix Binder, and Guilherme Fiusa for fruitful discussions. P. P. P. acknowledges funding from the Swiss National Science Foundation (Eccellenza Professorial Fellowship PCEFP2_194268). This material is based upon work supported by the U.S. Department of Energy, Office of Science, Office of Basic Energy Sciences under Award No. DE-SC0025516.

[1] F. Binder, L. A. Correa, C. Gogolin, J. Anders, and G. Adesso, *Thermodynamics in the Quantum Regime: Fundamental Aspects and New Directions*, Fundamental Theories of Physics Vol. 195 (Springer International Publishing, New York, 2018).
[2] R. Kosloff and A. Levy, Annu. Rev. Phys. Chem. **65**, 365 (2014).
[3] S. Bhattacharjee and A. Dutta, Eur. Phys. J. B **94**, 239 (2021).
[4] M. T. Mitchison, Contemp. Phys. **60**, 164 (2019).
[5] S. Vinjanampathy and J. Anders, Contemp. Phys. **57**, 545 (2016).
[6] W. Niedenzu, M. Huber, and E. Boukobza, Quantum **3**, 195 (2019).
[7] K. Hammam, Y. Hassouni, R. Fazio, and G. Manzano, New J. Phys. **23**, 043024 (2021).
[8] A. Roulet, S. Nimmrichter, J. M. Arrazola, S. Seah, and V. Scarani, Phys. Rev. E **95**, 062131 (2017).
[9] W. Pauli, *Festschrift zum 60. Geburtstage A. Sommerfeld* (Hirzel, Leipzig, 1928).
[10] U. Seifert, Annu. Rev. Condens. Matter Phys. **10**, 171 (2019).
[11] R. J. Harris and G. M. Schütz, J. Stat. Mech. (2007) P07020.
[12] H. Carmichael, *An Open Systems Approach to Quantum Optics*, 1st ed., Lecture Notes in Physics Monographs (Springer, Berlin, Heidelberg, 1993).
[13] J. Dalibard, Y. Castin, and K. Mølmer, Phys. Rev. Lett. **68**, 580 (1992).
[14] J. P. Garrahan and I. Lesanovsky, Phys. Rev. Lett. **104**, 160601 (2010).
[15] B. Donvil and P. Muratore-Ginanneschi, Nat. Commun. **13**, 4140 (2022).
[16] H.-P. Breuer, Phys. Rev. A **68**, 032105 (2003).
[17] K. Mølmer, Y. Castin, and J. Dalibard, J. Opt. Soc. Am. B **10**, 524 (1993).
[18] F. W. J. Hekking and J. P. Pekola, Phys. Rev. Lett. **111**, 093602 (2013).
[19] G. Manzano and R. Zambrini, AVS Quantum Sci. **4**, 025302 (2022).
[20] B. Leggio, A. Napoli, A. Messina, and H.-P. Breuer, Phys. Rev. A **88**, 042111 (2013).
[21] H. M. Wiseman and G. J. Milburn, *Quantum Measurement and Control* (Cambridge University Press, Cambridge, England, 2009).
[22] M. B. Plenio and P. L. Knight, Rev. Mod. Phys. **70**, 101 (1998).
[23] G. T. Landi, M. J. Kewming, M. T. Mitchison, and P. P. Potts, PRX Quantum **5**, 020201 (2024).
[24] A. Hofmann, V. F. Maisi, C. Gold, T. Krähenmann, C. Rössler, J. Basset, P. Märki, C. Reichl, W. Wegscheider, K. Ensslin, and T. Ihn, Phys. Rev. Lett. **117**, 206803 (2016).

[25] Z. K. Minev, S. O. Mundhada, S. Shankar, P. Reinhold, R. Gutiérrez-Jáuregui, R. J. Schoelkopf, M. Mirrahimi, H. J. Carmichael, and M. H. Devoret, Nature (London) **570**, 200 (2019).
[26] W. Chen, M. Abbasi, Y. N. Joglekar, and K. W. Murch, Phys. Rev. Lett. **127**, 140504 (2021).
[27] J. C. Bergquist, R. G. Hulet, W. M. Itano, and D. J. Wineland, Phys. Rev. Lett. **57**, 1699 (1986).
[28] J. Bylander, T. Duty, and P. Delsing, Nature (London) **434**, 361 (2005).
[29] T. Fujisawa, T. Hayashi, Y. Hirayama, H. D. Cheong, and Y. H. Jeong, Appl. Phys. Lett. **84**, 2343 (2004).
[30] T. Fujisawa, T. Hayashi, R. Tomita, and Y. Hirayama, Science **312**, 1634 (2006).
[31] S. Gleyzes, S. Kuhr, C. Guerlin, J. Bernu, S. Deléglise, U. Busk Hoff, M. Brune, J.-M. Raimond, and S. Haroche, Nature (London) **446**, 297 (2007).
[32] S. Gustavsson, R. Leturcq, B. Simovič, R. Schleser, T. Ihn, P. Studerus, K. Ensslin, D. C. Driscoll, and A. C. Gossard, Phys. Rev. Lett. **96**, 076605 (2006).
[33] S. Gustavsson, R. Leturcq, M. Studer, I. Shorubalko, T. Ihn, K. Ensslin, D. Driscoll, and A. Gossard, Surf. Sci. Rep. **64**, 191 (2009).
[34] W. Lu, Z. Ji, L. Pfeiffer, K. W. West, and A. J. Rimberg, Nature (London) **423**, 422 (2003).
[35] Z. Gong, Y. Ashida, and M. Ueda, Phys. Rev. A **94**, 012107 (2016).
[36] G. D. Chiara, G. Landi, A. Hewgill, B. Reid, A. Ferraro, A. J. Roncaglia, and M. Antezza, New J. Phys. **20**, 113024 (2018).
[37] R. D. Mayrhofer, C. Elouard, J. Splettstoesser, and A. N. Jordan, Phys. Rev. B **103**, 075404 (2021).
[38] J. Monsel, M. Acciai, R. Sánchez, and J. Splettstoesser, Phys. Rev. B **111**, 045419 (2025).
[39] M. Esposito, U. Harbola, and S. Mukamel, Phys. Rev. B **75**, 155316 (2007).
[40] T. Brandes, Ann. Phys. (Berlin) **520**, 477 (2008).
[41] M. Campisi, P. Hänggi, and P. Talkner, Rev. Mod. Phys. **83**, 771 (2011).
[42] M. Esposito, U. Harbola, and S. Mukamel, Rev. Mod. Phys. **81**, 1665 (2009).
[43] U. Seifert, Rep. Prog. Phys. **75**, 126001 (2012).
[44] C. Jarzynski and D. K. Wójcik, Phys. Rev. Lett. **92**, 230602 (2004).
[45] C. Jarzynski, Annu. Rev. Condens. Matter Phys. **2**, 329 (2011).
[46] D. Andrieux, P. Gaspard, T. Monnai, and S. Tasaki, New J. Phys. **11**, 043014 (2009).
[47] M. Campisi, J. Phys. A **47**, 245001 (2014).
[48] M. Campisi, J. Pekola, and R. Fazio, New J. Phys. **17**, 035012 (2015).
[49] H. J. D. Miller, M. H. Mohammady, M. Perarnau-Llobet, and G. Guarnieri, Phys. Rev. E **103**, 052138 (2021).
[50] J. P. Garrahan and I. Lesanovsky, Phys. Rev. Lett. **104**, 160601 (2010).
[51] B. Karimi and J. P. Pekola, Phys. Rev. Lett. **124**, 170601 (2020).
[52] P. Menczel, C. Flindt, and K. Brandner, Phys. Rev. Res. **2**, 033449 (2020).
[53] W. G. van der Wiel, S. De Franceschi, J. M. Elzerman, T. Fujisawa, S. Tarucha, and L. P. Kouwenhoven, Rev. Mod. Phys. **75**, 1 (2002).
[54] H. Thierschmann, M. Henke, J. Knorr, L. Maier, C. Heyn, W. Hansen, H. Buhmann, and L. W. Molenkamp, New J. Phys. **15**, 123010 (2013).
[55] H. Thierschmann, R. Sánchez, B. Sothmann, F. Arnold, C. Heyn, W. Hansen, H. Buhmann, and L. W. Molenkamp, Nat. Nanotechnol. **10**, 854 (2015).
[56] G. Jaliel, R. K. Puddy, R. Sánchez, A. N. Jordan, B. Sothmann, I. Farrer, J. P. Griffiths, D. A. Ritchie, and C. G. Smith, Phys. Rev. Lett. **123**, 117701 (2019).
[57] W. Khan, P. P. Potts, S. Lehmann, C. Thelander, K. A. Dick, P. Samuelsson, and V. F. Maisi, Nat. Commun. **12**, 5130 (2021).
[58] V. Blickle and C. Bechinger, Nat. Phys. **8**, 143 (2012).
[59] J.-W. Zhang, J.-Q. Zhang, G.-Y. Ding, J.-C. Li, J.-T. Bu, B. Wang, L.-L. Yan, S.-L. Su, L. Chen, F. Nori, Ş. K. Özdemir, F. Zhou, H. Jing, and M. Feng, Nat. Commun. **13**, 6225 (2022).
[60] V. Gorini, A. Kossakowski, and E. C. G. Sudarshan, J. Math. Phys. (N.Y.) **17**, 821 (1976).
[61] G. Lindblad, Commun. Math. Phys. **48**, 119 (1976).
[62] A. Levy and R. Kosloff, Phys. Rev. Lett. **108**, 070604 (2012).
[63] E. A. Martinez and J. P. Paz, Phys. Rev. Lett. **110**, 130406 (2013).
[64] L. A. Correa, J. P. Palao, D. Alonso, and G. Adesso, Sci. Rep. **4**, 3949 (2014).
[65] G. Maslennikov, S. Ding, R. Hablützel, J. Gan, A. Roulet, S. Nimmrichter, J. Dai, V. Scarani, and D. Matsukevich, Nat. Commun. **10**, 202 (2019).
[66] S. K. Manikandan, E. Jussiau, and A. N. Jordan, Phys. Rev. B **102**, 235427 (2020).
[67] See Supplemental Material at http://link.aps.org/supplemental/10.1103/PhysRevLett.134.150402, which includes Refs. [68,69], for the proof on single excitations constraining the form of master equations, derivations of cycle probabilities, connections from statistics of jumps to familiar quantities from full counting statistics, probabilities of idle cycles and their time intervals between two useful cycles, and technical details on the three-level masers.
[68] R. A. Horn and C. R. Johnson, *Matrix Analysis* (Cambridge University Press, Cambridge, England, 1985), p. 157.
[69] K. Prech, G. T. Landi, F. Meier, N. Nurgalieva, P. P. Potts, R. Silva, and M. T. Mitchison, arXiv:2406.19450.
[70] J. A. Almanza-Marrero and G. Manzano, arXiv:2403.19280.
[71] A. A. S. Kalaee, A. Wacker, and P. P. Potts, Phys. Rev. E **104**, L012103 (2021).
[72] Alternatively, it could also represent an accelerator, wherein the direction of heat flow remains the same, but work is injected instead of extracted. For simplicity, we will continue to refer to this as a work cycle. This scenario always holds when the energy exchanged with the cold bath is smaller than that with the hot bath, an assumption we make implicitly.
[73] G. T. Landi, arXiv:2305.07957.
[74] I. D. Terlizzi and M. Baiesi, J. Phys. A **52**, 02LT03 (2018).
[75] T. Nishiyama and Y. Hasegawa, Phys. Rev. E **109**, 044114 (2024).

[76] H. E. D. Scovil and E. O. Schulz-DuBois, Phys. Rev. Lett. **2**, 262 (1959).
[77] E. Boukobza and D. J. Tannor, Phys. Rev. A **74**, 063822 (2006).
[78] L. M. Cangemi, C. Bhadra, and A. Levy, Phys. Rep. **1087**, 1 (2024).
[79] J. Liu and D. Segal, Phys. Rev. E **103**, 032138 (2021).
[80] V. Singh, Phys. Rev. Res. **2**, 043187 (2020).
[81] E. Geva and R. Kosloff, Phys. Rev. E **49**, 3903 (1994).
[82] E. Boukobza and D. J. Tannor, Phys. Rev. Lett. **98**, 240601 (2007).
[83] P. Pietzonka and U. Seifert, Phys. Rev. Lett. **120**, 190602 (2018).